Inverted Base Pavement in LaGrange, Georgia: Characterization and Preliminary Numerical Analyses

Douglas D. Cortes
New Mexico State University
(formerly Georgia Tech)
dcortes@nmsu.edu
(Corresponding Author*)

J. Carlos Santamarina
Georgia Institute of Technology
jcs@gatech.edu

*Civil Engineering Department
New Mexico State University
Las Cruces, NM 88003-8001
Phone: 404.246.1969

Text Word Count: 4,009

- Abstract: 172
- Introduction: 388
- Body: 2,471
- Conclusions: 305
- References: 673

Tables: 1 x 250 = 250
Figures: 6 x 250 = 1,500

Total: **5,759**

ABSTRACT

A comprehensive experimental study was conducted during the construction of a full-scale inverted pavement test section in LaGrange, Georgia. Inverted base pavements consist of an unbound aggregate base placed between a stiff cement-treated foundation layer and a thin asphalt cover. Unlike conventional pavements which rely on upper stiff layers to bear and spread traffic loads, the unbound aggregate inter-layer in an inverted base pavement plays a major role in the mechanical response of the pavement structure. Given the critical role of the unbound aggregate base and its proximity to the surface, special attention was placed to monitoring changes in the material behavior induced by compaction over the stiff cement-treated base and to characterize the stress dependent stiffness of the compacted aggregate. A detailed study of all layers was conducted along the test section before, during and after construction to gain critically needed information to enhance our understanding of the internal behavior and macro-scale performance of inverted pavement structures. The information compiled during the field test was used in a complementary numerical study.

INTRODUCTION

The need for improved road performance, optimal use of resources, budget constraints, and energy efficiency prompt the analysis of alternative pavement structures. Inverted base pavements have been used as affordable and structurally competent pavement structures in South Africa since the 1950's (*1*, *2*, *3*). The South African flexible pavement design emphasizes the importance of a good foundation, and involves novel construction methods and careful material selection to achieve dense unbound aggregate layers that exhibit a remarkable ability to support the heaviest traffic loads under both dry and wet conditions (*1*). The unbound aggregate layer is compacted on top of a cement-treated base to provide a suitable foundation, both during compaction and throughout the service life (*4*). While stabilized layers alone improve the structural capacity of the pavement they may cause reflective cracking, which accelerates pavement deterioration. Yet, a stone inter-layer can prevent the propagation of reflective cracks through strain dissipation within the unbound aggregate layer (*5*). Both, the South African experience and the accumulating experience in the U.S.A. show that inverted base pavements may outperform conventional flexible pavement structures (*5*, *6*, *7*, *8*, *9*, *10*, *11*).

The use of inverted base pavements in the U.S.A. has been hindered by the lack of field experiments and related research required to investigate the mechanical response of this pavement structure under local conditions, construction practices, and required quality control and performance. A full-scale field study was conducted in LaGrange, Georgia, in collaboration with the Georgia Department of Transportation (GDOT – see companion paper *12*). The laboratory and field studies conducted as part of this pilot project and complementary analyses advance both the current state of knowledge on the behavior of inverted base pavement systems and the state of the practice in terms of construction processes and quality assurance.

The study documented herein was designed to gather detailed information before, during and after the construction of the inverted base pavement test section at LaGrange, in order to gain critically needed understanding of the internal behavior and macro-scale performance of this pavement structure through complementary analytical and numerical studies. Details can be found in *13*.

PROJECT DESCRIPTION

The test section is part of an industrial parkway intended to serve the growing car manufacturing industry in south-west Georgia. The inverted base pavement test section is a two-lane 1,036m long stretch of the south LaGrange loop. It was designed to sustain an initial one-way annual average traffic of 7,000 vehicles per day projected to grow to 11,700 by the end of its service life. Truck traffic is estimated at 7% and consists of 3% multi-unit (truck tractor semi-trailers and full trailer combination vehicles) and 4% single-unit (two and three axle trucks and busses having six tires). The Georgia DOT designed the rigid pavement following the AASHTO (1972) interim pavement design guide; the inverted base pavement was designed using empirical guidelines from the South African experience. The structural comparison between the conventional rigid pavement and the inverted section could not be made a priori.

The test section cuts across residual soils from the Georgia Piedmont geologic formation. Figure 1a shows the original topography and the built longitudinal cross section. Material removed from the cut sections was transported and compacted in the two fill sections. Construction of the subgrade took place from 1/7/2008 to 2/19/2008. The upper 0.15 m of the subgrade were stabilized by mixing in crushed stone and compacting. Stabilization work began on 7/23/2008 and was completed on 7/30/2008.

The construction of the cement-treated base took place between 7/30/2008 and 8/5/2008. Cement and aggregate were mixed in a pug mill and hauled 3.2 km to the construction site. Spreading and compaction operations started at station 280+00 and moved along the westbound lane towards station 314+00. The eastbound lane was constructed on the way back, from station 314+00 towards station 280+00. Construction issues near the bridge approach (station 314+00) lead to a short gap in the test section near the bridge. The mix contained 4% cement by weight and was compacted to 98% of Proctor. Progress was monitored from the time the cement treated aggregate left the pug mill until the final bituminous seal coat was placed.

The placement and compaction of the unbound aggregate base started 8/11/2008 and lasted 18 days. The asphalt concrete layer was placed in two lifts. The first was a 19 mm NMS 0.05 m thick layer built shortly after the completion of the unbound aggregate base in 10/16/2008. The riding surface was a 12.5 mm NMS, 0.04 m thick added on 4/18/2009.

LABORATORY AND FIELD MATERIAL CHARACTERIZATION

The layers were carefully monitored during construction, including extensive material characterization in the laboratory and in the field. Results are summarized in Table 1.

Subgrade

Thirty five subgrade samples were collected from the test section and used to determine grain size distribution, specific surface, liquid limit, bulk density, water content, complex permittivity, electrical conductivity, suction, and P-wave velocity in the laboratory. The field characterization of the subgrade included dynamic cone penetrometer, helical probe test and surface waves. Test results are summarized in table 1, the main findings follow.

The mean grain size distribution is characterized by D_{10} = 0.2 mm, D_{50} = 0.5 mm, coefficient of uniformity C_u = 6, and coefficient of curvature C_c = 1.3, which are characteristic of well graded granular materials. The fraction of fines (d<75μm) ranged from 1% (at station 299+00) to 36% (at station 306+00). The high specific surface of the fine fraction suggested the presence of clay minerals (7 to 30 $m^2 \cdot g^{-1}$), and susceptibility to changes in water content and/or pore fluid chemistry.

TABLE 1 Laboratory and Field Material Characterization

Layer (thickness)	**Parameter**	**Measured Value**
Asphalt Concrete (89 mm)	Surface Wave Velocity V_R [m·s^{-1}] P-wave Velocity V_p [m·s^{-1}]	1,000 ~ 2,400 3,500 ~ 4,100
Unbound Aggregate Base (158 mm)	Surface Wave Velocity V_R [m·s^{-1}]	200 ~ 300
Cement Treated Base (254 mm)	Electrical Resistivity $\rho_{electric}$ [Ω·m] P-wave Velocity V_p [m·s^{-1}] Surface Wave Velocity V_R [m·s^{-1}] Compressive Strength σ [MPa]	800 ~ 5000 2,900 ~ 3,400 1,400 ~ 1,900 3 ~ 5
Stabilized Subgrade (158 mm)	Surface Waves V_R [m·s^{-1}]	200 ~ 300
Subgrade (< 12 m)	Coef. Uniformity C_u & Curvature C_c Fraction smaller than 75μm [ ] D_{10} [mm] Specific Surface S_s [m^2·g^{-1}] Liquid Limit LL [%] Water Content w [%] Penetration Rate PR [mm·blow^{-1}] Torque (HPT) T [N·m] Porosity n [ ] Matric Suction h_M [kPa] Osmotic Suction h_π [kPa] P-wave Velocity V_p [m·s^{-1}] Surface Waves V_R [m·s^{-1}]	6 & 1.3 0.012 ~ 0.36 0.09 ~ 0.25 7 ~ 30 50 ~ 100 15 ~ 40 4 ~ 15 5 ~ 12 0.3 ~ 0.5 50 ~ 500 100 ~ 1,000 300 ~ 800 150 ~ 200

The recovered in-situ water content data fall within the range of optimum water content established by Proctor compaction tests carried out by GDOT. Measured liquid limit values are plotted in figure 1b for reference. Total suction data gathered at the in-situ water content fall between 200 and 1,500 kPa. Similar results are observed in the matric and osmotic suction measurements. Even higher suctions are anticipated at lower water contents under dry climate conditions. The measured suction levels anticipate a high moisture-dependent response of the subgrade.

The P-wave velocity in unsaturated sediments is practically unaffected by the bulk stiffness of the fluid when the degree of saturation S≤95%. Instead, it reflects the stiffness of the soil skeleton which is in part controlled by capillary forces, i.e. suction (*14*). Measured P-wave velocities for the subgrade are in the range from 300 to 800 m·s^{-1}, in agreement with the high measured suction values, which suggest that capillarity controls the subgrade stiffness. It should be noted that only samples that satisfied the test geometrical constraints where used to determine V_p. Since the soil samples that fulfilled this requirement where for the most part very well compacted blocks, the measurement is biased to stiffer values and does not necessarily represent the average stiffness of the subgrade. The field-measured surface wave velocities range from V_R = 150 to 200 m·s^{-1}.

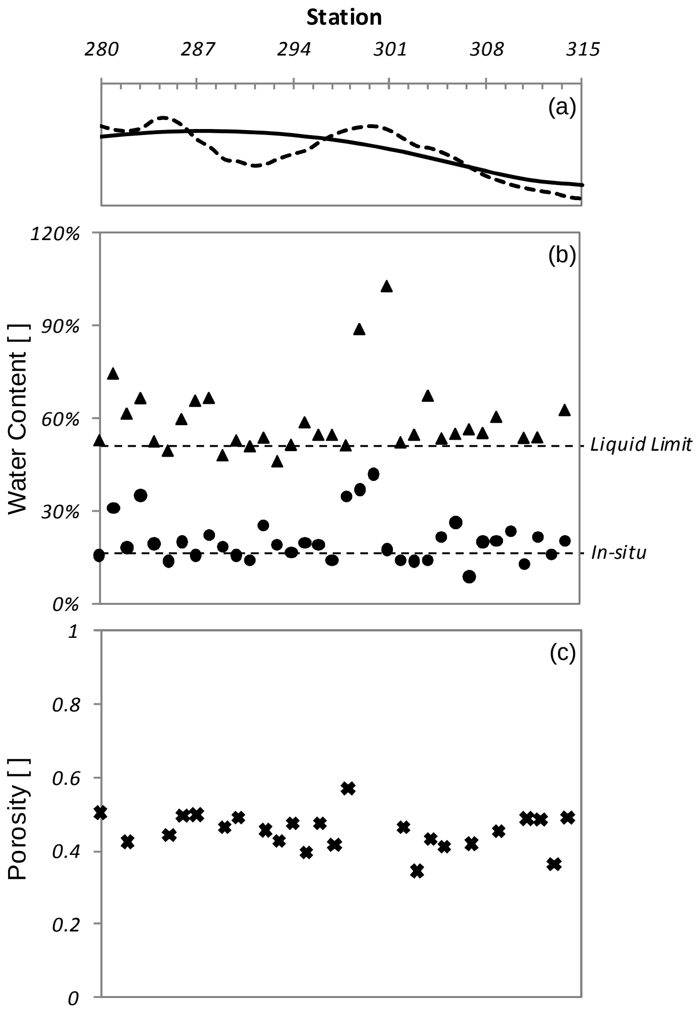

FIGURE 1 Topography and Subgrade. (a) original topography (dashed line) and as-built longitudinal cross section showing cut and fill zones. The subgrade was characterized after compaction; samples recovered at every station were used to determine (b) liquid limit (filled triangles), in-situ water content (filled circles), and (c) porosity.

The measured helical probe torque and dynamic cone penetration resistance are positively correlated to both the total suction and the dry density; no evident correlation with bulk density or porosity was observed. Dynamic cone penetration data can be used in conjunction with density, liquid limit, and water content to estimate the resilient modulus of the subgrade (*15*)

$$E_R = a_o (PR)^{a_1} \left[\gamma_{dry}^{a_2} + \left(\frac{LL}{w_c} \right)^{a_3} \right] \qquad \text{(i)}$$

where *PR* is the dynamic cone penetration rate, γ_{dry} is the dry unit weight, *LL* is the liquid limit, w_c is the water content, and a_i are fitting parameters. The estimated resilient modulus is E_R = 250 MPa with a standard deviation of 100 MPa.

Cement-Treated Base

The off-site mixing, transport, spreading, and compaction of the cement-treated base were carefully monitored to assess hydration prior to compaction. Electrical properties of curing cementitious materials vary as a function of hydration, pore fluid composition, moisture, and temperature (*16*, *17*, *18*, *19*, *20*, *21*, *22*). As the cement paste cures in a mortar mixture there is a reduction in the ionic concentration of the pore fluid which leads to measurable changes in electrical resistivity. Therefore, electrical resistivity data can be used to assess the curing evolution of Portland cement mixtures. Curing of the compacted material was monitored using an electrical resistivity probe developed as part of this study. Different locations near the spreader were selected and tested in order to assess spatial variability and to detect heterogeneities. Results show no significant resistivity difference from location to location, suggesting homogeneity in the construction process. After collection of spatial variability data, the electrical resistivity monitoring equipment was fixed at a given location to monitor the time evolution of electrical resistance with time, which can be used as an index of curing progress. Resistivity measurements started approximately 20 to 30 minutes after the cement was first exposed to water in the mixer. Field data show noticeable changes in conductivity starting at 100 min (figure 2).

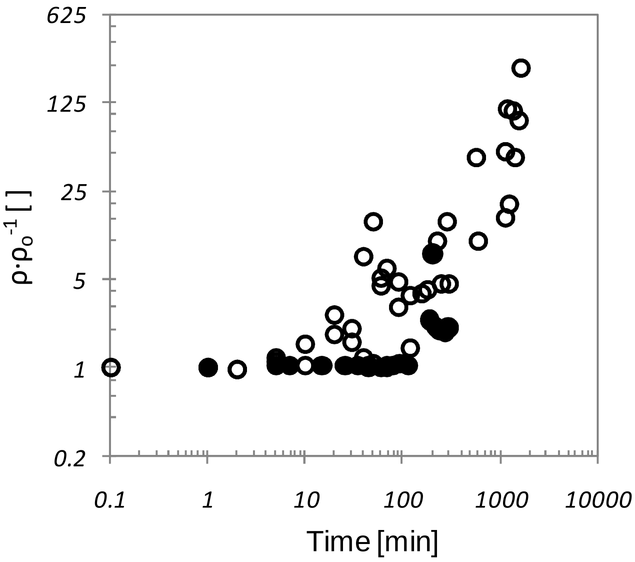

FIGURE 2 Cement Treated Base. Curing was monitored using a 4-electrode probe to determine electrical resistivity. Similar preliminary tests were conducted in the laboratory. Field data (filled circles) show an increase in resistivity starting at 100 min; laboratory specimens exhibit resistivity increases as early as 20 min after mixing (hollow circles).

Characterization of the hardened cement-treated base properties was done on 7-day cores recovered from the site and tested for laboratory P-wave velocity and compressive strength; a summary of results is presented in table 2.3. A primary concern with the construction of the inverted base pavement structure is the mechanical response of the cement-treated base during the compaction of the unbound layer above and its long-term integrity. Copper wire loops were installed within the cement-treated base surface at selected locations. A 6.35 mm thick groove was cut 12.7 mm into the sub-base. Then, a thin polyurethane coated copper wire d = 0.3 mm was placed in the grove and bonded to the sub-base using mortar mix. The resistance between the two ends was measured immediately after the installation of the wire to verify its integrity. The resistance at each of the three instrumented stations was measured following the construction of the unbound aggregate base; no changes from the pre-construction values were observed. These results show that the cement-treated base sustained no significant damage during the compaction of the unbound aggregate and the asphalt concrete layers. This was later confirmed in a forensic study through visual inspection.

Unbound Aggregate Base

The unbound aggregate base is the central component of the inverted base pavement structure. Therefore, special attention was devoted to identify changes in the aggregate base properties caused by compaction over the stiff cement-treated base. Aggregate samples were recovered pre and post compaction to determine grain size distribution in an effort to establish if crushing was taking place during compaction. Findings of the gradation tests are summarized in figure 3a. Overall the data remain inconclusive as to the extent and significance of particle crushing.

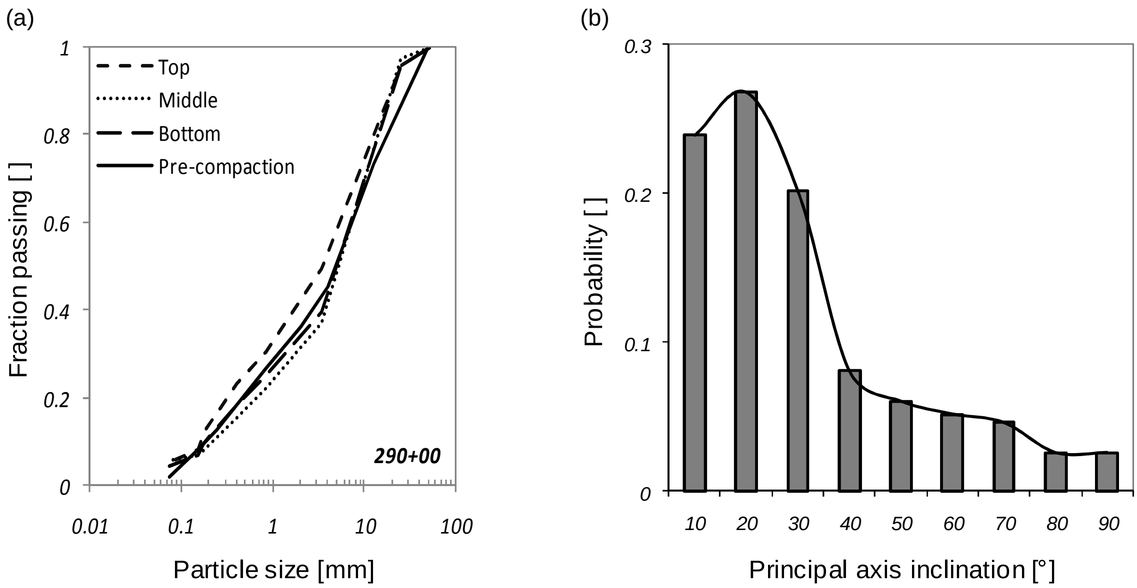

FIGURE 3 Unbound Aggregate Base. (a) Changes in grain size distribution - sample recovered at station 290+00. (b) Preferential particle orientation from digital image processing of photographs taken during the forensic investigation.

The development of inherent anisotropy in the unbound aggregate layer as a result of compaction induced particle alignment was assessed via a forensic study. Trenches were dug through the asphalt layer uncovering the unbound aggregate and allowing us to take a look inside the unbound aggregate base and photograph the grain skeleton. Digital image analysis results presented in figure 3b show that particles preferentially align with their major axis parallel to the horizontal plane. Note that only the coarser visible particles are considered in this analysis.

The as-built unloaded stiffness of the unbound aggregate base was determined using spectral analysis of surface waves (SASW) prior to the construction of the asphalt concrete layer. The unbound aggregate non-linear stiffness-stress response is critical to the mechanical response of an inverted pavement structure; therefore, the stiffness-stress relationship of the unbound aggregate was determined using a novel laboratory procedure to simultaneously determine the stress-dependent vertical and radial stiffness. The unbound aggregate base material is mixed at the optimum water content, placed in a Proctor-type mold, and compacted in a vibratory table for 15 minutes under a 240 N weight i.e., a vertical stress of 13 kPa. Two holes are drilled though the compacted material to allow for the installation of the source and receiver arrays. The instrumented cell is placed in the loading frame and the sensors are connected to the peripheral electronics. Signals picked up by the array of receivers are pre-amplified, filtered to remove high frequency noise, digitized using 4-channel oscilloscope, and stored into a laptop computer.

The specimen undergoes 25 cycles of preconditioning loading-and-unloading with vertical stress amplitude of 700 kPa. The unloading after the final cycle is stopped at a vertical stress of 14 kPa to simulate the overburden on the unbound aggregate base. The first measurements are made starting at 14 kPa and every 80 kPa until the vertical stress is 580 kPa which is 83% of the maximum preconditioning vertical stress. The set of signals recorded at each load increment presented in figure 4b shows the strong stress dependency of unbound aggregates. These laboratory results and complementary field measurements allowed us to calibrate physically appropriate and simple stiffness-stress expressions of the following form (*23*):

$$E_R = k_1\left(\frac{p}{p_0}\right)^{k_2}\left[1-k_3\left(\frac{q}{q_f}\right)^{k_4}\right] \qquad \text{(ii)}$$

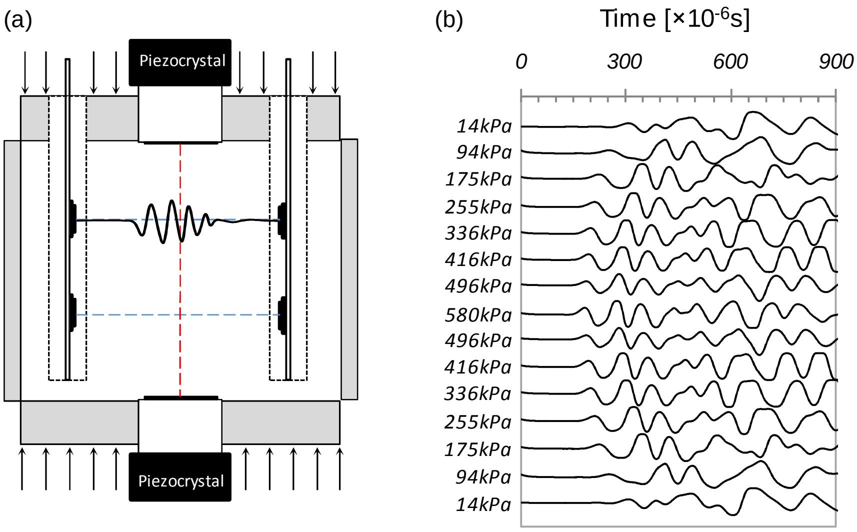

FIGURE 4 Unbound Aggregate Base: Stress-dependent stiffness. (a) Instrumented laboratory zero lateral strain test cell. (b) Signature cascades as a function of the applied vertical stress clearly show shorter travel times at higher stress.

Asphalt Concrete

The characterization of the asphalt layer focused on the determination of elastic parameters, namely the elastic modulus and the Poisson's ratio. This was accomplished through field measurements of surface waves and laboratory P-wave velocity measurements in samples recovered during the forensic investigation.

These data are used to estimate the constrained modulus M using theory of elasticity and assuming isotropic stiffness; for example, given field velocity data V_R and the measured bulk densities ρ,

$$M \approx 2\rho\left(\frac{V_R}{0.9}\right)^2 \frac{(1-\nu)}{(1-2\nu)} \qquad \text{(iii)}$$

The constrained modulus computed from measurements gathered along the test section is summarized in figure 5; the figure includes stiffness data determined for all layers (without load).The stiffness profile of the as-built pavement structure -without load- ranges from 30,000 MPa for the asphalt concrete to 140 MPa for the subgrade.

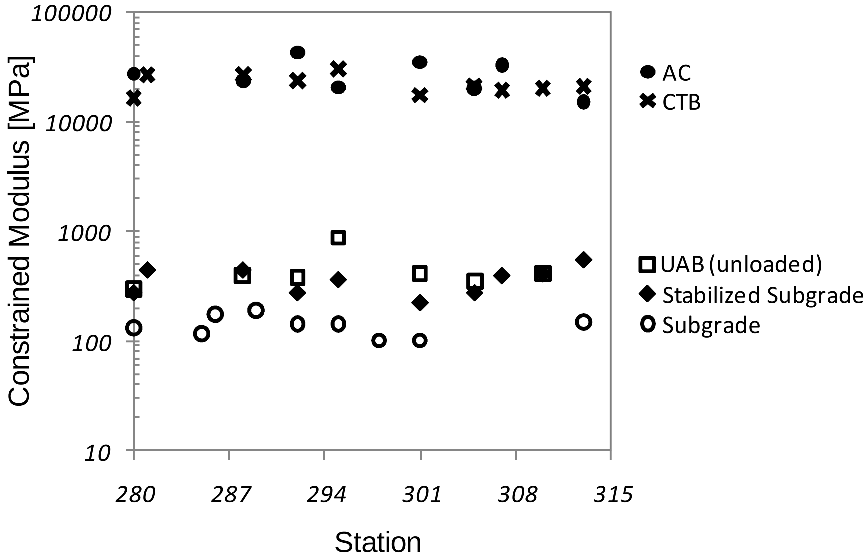

FIGURE 5 Asphalt Concrete: Stiffness. Wave propagation velocity was determined for each layer using high-resolution SASW. All measurements summarized in this figure show the high stiffness of the AC and CTB layers (low stress sensitivity) compared to the aggregate base and the subgrade (stress-dependent – values shown are without load).

PRELIMINARY ANALYSES – NUMERICAL SIMULATION

The inverted base pavement was modeled using the finite element software ABAQUS. In these simulations, the asphalt concrete, AC, and cement treated base, CTB, were modeled as elastic media. The unbound aggregate base, UAB, and the subgrade, SG, were modeled as cross-isotropic, non-linear elastoplastic materials, in agreement with equation 2 (Note: the stress-dependent stiffness is extracted from laboratory data such as figure 4b, and complementary field data). The subroutine was written in Fortran and implemented in ABAQUS (details in *13*). The tire-pavement system was modeled using a 3D axisymmetric mesh, with zero-lateral-displacement boundaries at the edge of the pavement, zero-vertical-displacement at the foundation of the structure, and no-slip between the layers.

The resulting vertical, radial and shear stress distributions along the centerline beneath the wheel are presented in figure 6a. Vertical stresses along the centerline are compressive throughout the full depth of influence of the load, and become negligible within the cement-treated base. Radial stresses range from compression at the top of the asphalt concrete and cement-treated base layers, to tension at the bottom. Both vertical and radial stresses in the unbound aggregate base remain in compression for the full depth of these layers (in agreement with Mohr-Coulomb behavior). Radial slices of the vertical stress field are shown at interfaces in figure 6b. The vertical stress caused by the wheel load diminishes with depth; the peak vertical stress on the subgrade is less than 5% of the vertical stress applied on the surface.

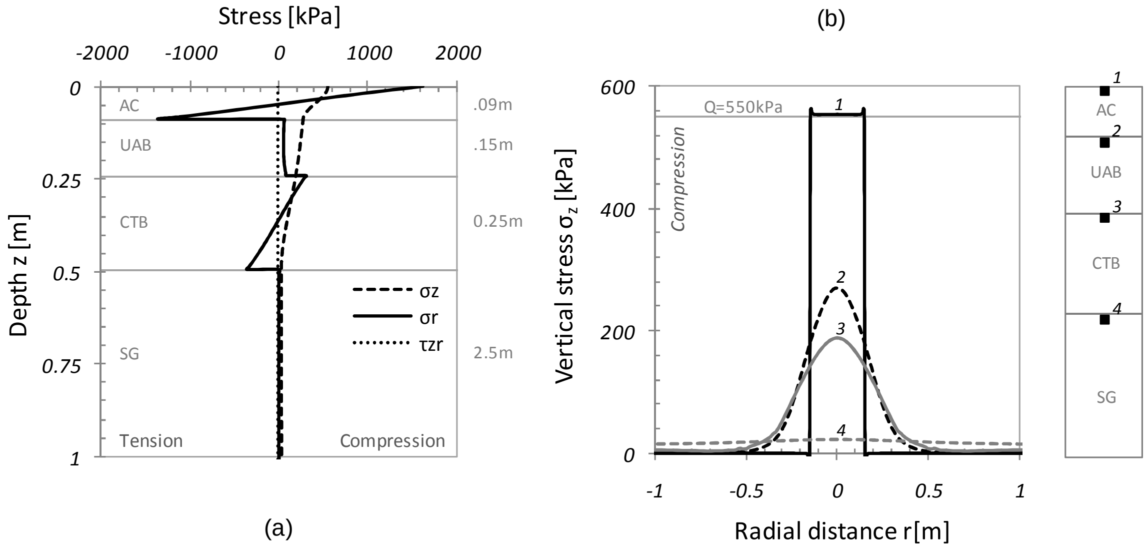

FIGURE 6 Induced stresses in an inverted base pavement beneath a wheel modeled as a 550 kPa uniformly distributed load over a circular area of radius 0.15 m. (a) Vertical σ_z, radial σ_r, and shear τ_{zr} stress profiles as a function of depth along the load centerline. (b) Radial profiles of induced vertical stresses at multiple locations within the inverted base pavement structure.

CONCLUSIONS

The full-scale inverted pavement test section in LaGrange, Georgia, offered a unique opportunity to characterize with unprecedented detail the properties of the different layers during construction. This information is of critical importance for the understanding of these pavement structures and to support numerical models and simulations.

The as-built inverted base pavement stiffness profile exhibits pronounced contrast among successive layers; 30,000 MPa at the asphalt concrete, 500 MPa for the unbound aggregate base (unloaded), 22,000 MPa for the cement-treated base, and 150MPa for the compacted subgrade. This unconventional high-low-high-low stiffness sequence is a salient characteristic of inverted base pavements.

The average measured specific surface and coefficient of uniformity of the subgrade at LaGrange indicate that its mechanical behavior is strongly influenced by electrical interactions and capillarity; therefore, the subgrade is susceptible to changes in water content and pore fluid chemistry. The high P-wave velocity values measured as part of this study reflect the high suction at the time of measurements.

The off-site mixing, followed by transport, spreading, and compaction of the cement-treated base resulted in a homogeneous layer. No early setting of the cement mixture was observed. The 7-day cured cement-treated base withstood without cracking the heavy compaction equipment used to attain high density in the overlaying unbound aggregate layer.

The unbound aggregate base stiffness is a non-linear function of the state of stresses. The stiffness-stress relationship can be adequately determined in instrumented zero-lateral-strain cells. Pre and post compaction gradation test results do not offer a clear assessment of the extent and significance of particle crushing in the unbound aggregate layer during compaction over the stiff cement-treated base. Digital image analysis confirmed particle alignment inducing inherent anisotropy in the as-built unbound aggregate base.

Preliminary numerical results obtained with proper material models for all layers confirm acceptable stresses in the various layers under the design traffic loads.

ACKNOWLEDGMENTS

Support for this research was provided by the Georgia Department of Transportation, Georgia Construction Aggregate Association, National Stone, Sand & Gravel Association (AFTRE), and the Goizueta Foundation. Special thanks to J. Cardosa (GCAA) for decisive support, to D. Lewis (GDOT) for facilitating all field operations, and to Dr. A. Jugo for insightful comments and suggestions during this research.

REFERENCES

1. Horne, D., G. Belancio, S. A. Carradine, S. Gaj, J. Hallin, N. Jackson, C. Jordan, D. Lucas and R. Zink. *South African Pavement and Other Highway Technologies and Practices*. Federal Highway Administration U.S. Department of Transportation, 1997.
2. Rust, F. C., J. P. Mahoney and J. B. Sorenson. *An International View of Pavement Engineering*. Bearing Capacity of Roads and Airfields. Trondheim, Norway, 1998.
3. Beatty, T. L., D. C. Jackson, D. A. Dawood, R. A. Ford, J. S. Moulthrop, G. D. Taylor, F. L. Danchetz, D. A. Blanck, J. M. Fay, D. S. Keough, L. M. Rodriguez, M. D. Voth and Z. L. Webb. *Pavement Preservation Technology in France, South Africa, and Australia*. Alexandria, VA, Office of International Programs, Federal Highway Administration, U.S. Department of Transportation, and the American Association of State Highway and Transportation Officials, 2002.
4. Jooste, F. J. and L. Sampson. *The Economic Benefits of HVS Development Work on G1 Base Pavement*. Lynn East, Department of Public Transport, Roads and Works Gauteng Provincial Government, 2005
5. Rasoulian, M., H. Titi, M. Martinez, B. Becnel and G. Keel. *Long Term Performance of Stone Interlayer Pavement*. Louisiana Transportation Research Center, Baton Rouge LA, 2001.
6. Ahlvin, R. G., W. J. Turnbull, J. P. Sale and A. A. *Maxwell. Multiple-Wheel Heavy Gear Load Pavement Tests*. U.S. Army Corps of Engineers, Vicksburg, Mississippi, 1971.
7. Barker, W. R., W. N. Brabston and F. C. Townsend. *An Investigation of the Structural Properties of Stabilized Layers in Flexible Pavement Systems*. U.S. Army Corps of Engineers, Vicksburg, Mississippi, 1973.
8. Grau, R. W. *Evaluation of Structural Layers in Flexible Pavement*. U.S. Army Corps of Engineers, Vicksburg, Mississippi,1973.
9. Barksdale, R. D. Performance of Crushed-Stone Base Courses. *Transportation Research Record*. Vol. 954, 1984, pp. 78-87.
10. Tutumluer, E. and R. D. Barksdale. Inverted Flexible Pavement Response and Performance. *Transportation Research Record*. Vol. 1482, 1995, pp. 102-110.
11. Rasoulian, M., B. Becnel and G. Keel. Stone Interlayer Pavement Design. *Transportation Research Record*. Vol. 1709, 2000, pp. 60-68.
12. Lewis, D.E., Ledford, K., Georges, T., Jared, D.M. Construction and Performance of

Inverted Pavements in Georgia. *Submitted to: Transportation Research Record* 2012.

13. Cortes, D.D. *Inverted Base Pavement Structures*, PhD Thesis, School of Civil and Environmental Engineering, Georgia Institute of Technology, 2010.
14. Santamarina, J. C., K. A. Klein and M. A. Fam. *Soils and Waves*. John Wiley & Sons, Ltd., New York, 2001.
15. George, K. P. and W. Uddin. *Subgrade Characterization for Highway Pavement Design*. Mississippi Department of Transportation Research Division, Jackson, MS, 2000.
16. Monfore, G. E. Electrical Resistivity of Concrete. *Journal of the PCA Research and Development Laboratories*. Vol. 10, No. 2, 1968, pp. 35.
17. Christensen, B. J., R. T. Coverdale, R. A. Olson, S. J. Ford, E. J. Garboczi, H. M. Jennings and T. O. Mason. Impedance Spectroscopy of Hydrating Cement-Eased Materials - Measurement, Interpretation, and Application. *Journal of the American Ceramic Society* Vol. 77, No. 11, 1994, pp. 2789-2804.
18. Fam, M. A. and J. C. Santamarina. Study of Clay-Cement Slurries with Mechanical and Electromagnetic Waves. *Journal of Geotechnical Engineering.* Vol. 122, No. 5, 1996, pp. 365-373.
19. McCarter, W. J. Monitoring the Influence of Water and Ionic Ingress on Cover-Zone Concrete Subjected to Repeated Absorption. *Cement Concrete and Aggregates*. Vol. 18, No. 1, 1996, pp. 55-63.
20. McCarter, W. J., H. Ezirim and M. Emerson. Properties of Concrete in the Cover Zone: Water Penetration, Sorptivity and Ionic Ingress. *Magazine of Concrete Research.* Vol. 48, No. 176, 1996, pp. 149-156.
21. Rajabipour, F. and J. Weiss. Electrical Conductivity of Drying Cement Paste. *Materials and Structures*. Vol. 40, No. 10, 2007, pp. 1143-1160.
22. Revil, A. and P. W. J. Glover. Theory of Ionic-Surface Electrical Conduction in Porous Media. *Physical Review B.* Vol. 55, No. 3, 1997, pp. 1757.
23. Van Niekerk, A. A., A. A. A. Molenaar and L. J. M. Houben. *Effect of Material Quality and Compaction on the Mechanical Behaviour of Base Course Materials and Pavement Performance*. 6th International Conference on Bearing Capacity of Roads, Railways and Airfields, Lisbon, Portugal, 2002.